SUPER-CONVERGENCE: VERY FAST TRAINING OF RESIDUAL NETWORKS USING LARGE LEARNING RATES

Anonymous authors
Paper under double-blind review

ABSTRACT

In this paper, we show a phenomenon, which we named "super-convergence", where residual networks can be trained using an order of magnitude fewer iterations than is used with standard training methods. One of the key elements of super-convergence is training with cyclical learning rates and a large maximum learning rate. Furthermore, we present evidence that training with large learning rates improves performance by regularizing the network. In addition, we show that super-convergence provides a greater boost in performance relative to standard training when the amount of labeled training data is limited. We also provide an explanation for the benefits of a large learning rate using a simplification of the Hessian Free optimization method to compute an estimate of the optimal learning rate. The architectures and code to replicate this work will be made available upon publication.

1 INTRODUCTION

It is widely accepted that training deep neural networks is a time consuming and computationally burdensome process, often taking from hours to weeks, which can be a bottleneck for research and deep neural network applications. In this paper, we build on the observation in Goodfellow et al. (2014) that stochastic gradient descent (SGD) can spend most of its training time navigating a flat region in a loss function valley. Specifically, we show that, for certain datasets, residual network architectures (He et al., 2016), and hyper-parameter values, using very large learning rates with the cyclical learning rate (CLR) method (Smith, 2015; 2017) can speed up training by an order of magnitude. Analogous to the phenomenon of super-conductivity that only happens in limited and specific circumstances, we named this phenomenon "super-convergence." We do not intend to suggest a universal training methodology for all deep networks but to identify and characterize a potentially powerful phenomenon.

Figure 1a provides a comparison of test accuracies from a super-convergence example and the result of a typical (piecewise constant) training regime for Cifar-10, both using a 56 layer residual network architecture (Resnet-56). The piecewise constant training regime reaches a peak accuracy of 91.2% after approximately 80,000 iterations, while the super-convergence method reaches a higher accuracy (92.4%) after only 10,000 iterations. Figure 1b shows the results for a range of CLR stepsize values, where training lasted only one cycle. This modified learning rate schedule achieves a higher final test accuracy (92.1%) than typical training (91.2%) after only 6,000 iterations. In addition, as the total number of iterations increases from 2,000 to 20,000, the final accuracy improves from 89.7% to 92.7%.

The contributions of this paper are:

1. We demonstrate the existence of a new phenomenon (super-convergence, the very fast training of residual networks using CLR) and systematically look at the limiting cases to determine the boundaries of where it occurs and where it does not.
2. We show evidence that large learning rates (LR) regularize the trained network and hypothesize that this regularization is what improves test accuracy when super-convergence occurs.

3. We provide support for using large learning rates through using a simplification of the second order, Hessian-free optimization method to estimate optimal learning rates.
4. We demonstrate that the effects of super-convergence are increasingly drastic when less labeled training data is available.

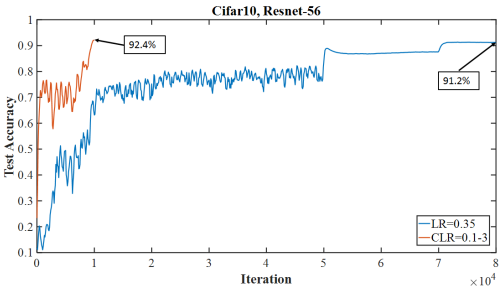

(a) Comparison of test accuracies of super-convergence example to a typical (piecewise constant) training regime.

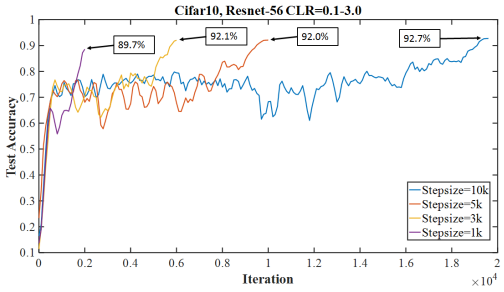

(b) Comparison of test accuracies of super-convergence for a range of stepsizes.

Figure 1: Examples of super-convergence with Resnet-56 on Cifar-10.

2 Background and Related Work

We are unaware of previous published work on the phenomenon we describe as super-convergence.

In this paper, when we refer to a typical, standard, or a piecewise-constant training regime, it means the practice of using a global learning rate, often near 0.1, for many epochs, until the test accuracy plateaus, and then continuing to train with a lower learning rate decreased by a factor of 0.1. This process of reducing the learning rate and continuing to train is often repeated two or three times.

There does exist extensive literature on stochastic gradient descent (SGD) (see Goodfellow et al. (2016) and Bottou (2012)) which is generally relevant to this work. Also, there exists a significant amount of literature on the loss function topology of deep networks (see Chaudhari et al. (2016) for a review of the literature). This paper contains a discussion of the loss function topology which follows from the work of Goodfellow et al. (2014) and subsequent work by Im et al. (2016) on characterizing the landscape. Methods for adaptive learning rates have also been an active area of research. This paper uses a simplification of the second order Hessian-Free optimization (Martens, 2010) to estimate optimal values for the learning rate. In addition, we utilize some of the techniques described in Schaul et al. (2013) and Gulcehre et al. (2017). Also, we show that adaptive learning rate methods such as Nesterov momentum (Sutskever et al., 2013; Nesterov, 1983), AdaDelta (Duchi et al., 2011), AdaGrad (Zeiler, 2012), and Adam (Kingma & Ba, 2014) do not use sufficiently large learning rates when they are effective nor do they lead to super-convergence without using CLR.

3 Super-convergence

In this work, we use cyclical learning rates (CLR) and the learning rate range test (LR range test) which were first suggested by Smith (2015) and later updated in Smith (2017). To use CLR, one specifies minimum and maximum learning rate boundaries and a stepsize. The stepsize is the number of iterations used for each step and a cycle consists of two such steps – one in which the learning rate increases and the other in which it decreases. Smith (2015) tested numerous ways to vary the learning rate between the two boundary values, found them to be equivalent and therefore recommended the simplest, which is letting the learning rate change linearly. We note that Loshchilov & Hutter (2016) independently proposed a similar method to CLR which they call SGDR. The SGDR method uses a sawtooth pattern with a cosine followed by a jump back up to the original value. Unfortunately, it is not possible to observe the super-convergence phenomenon when using this pattern. Our experiments show that training must begin with a small initial learning rate to enable super-convergence.

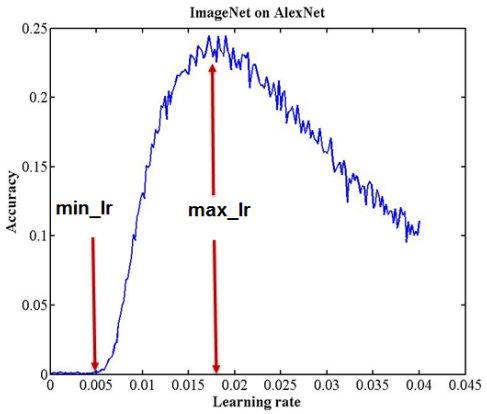

(a) Typical learning rate range test result where there is a peak to indicate max_lr.

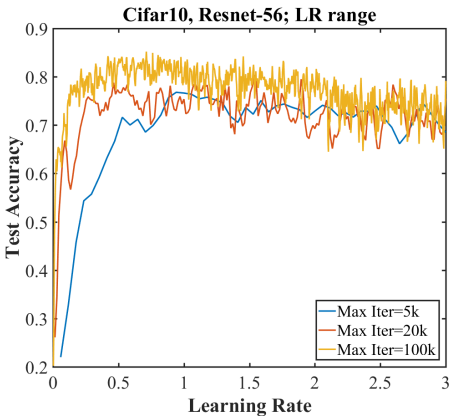

(b) Learning rate range test result with the Resnet-56 architecture on Cifar-10.

Figure 2: Comparison of learning rate range test results.

The LR range test can be used to determine if super-convergence is possible for an architecture. In the LR range test, training starts with a zero or very small learning rate which is slowly increased linearly throughout a pre-training run. This provides information on how well the network can be trained over a range of learning rates. Figure 2a shows a typical curve from a LR range test, where the test accuracy has a distinct peak.[1] When starting with a small learning rate, the network begins to converge and, as the learning rate increases, it eventually becomes too large and causes the training/test accuracy to decrease. The learning rate at this peak is the largest value to use as the maximum learning rate bound when using CLR. The minimum learning rate can be chosen by dividing the maximum by a factor of 3 or 4. The optimal initial learning rate for a typical (piecewise constant) training regime usually falls between these minimum and maximum values.

If one runs the LR range test for Cifar-10 on a 56 layer residual networks, one obtains the curves shown in Figure 2b. Please note that learning rate values up to 3.0 were tested, as opposed to a value on the order of 0.3, as would typically be used. The test accuracy remains consistently high over this unusually long range of large learning rates. This unusual behavior motivated our experimentation with much higher learning rates, and we believe that such behavior during a LR range test is indicative of potential for super-convergence. The three curves in this figure are for runs with a maximum number of iterations of 5,000, 20,000, and 100,000, where the test accuracy remains consistently high for a long range of large learning rate values.

Figure 3a provides an example of transversing the loss function topology.[2] This figure helps give an intuitive understanding of how super-convergence happens. The blue line in the Figure represents the trajectory of the training while converging and the x's indicate the location of the solution at each iteration and indicates the progress made during the training. In early iterations, the learning rate must be small in order for the training to make progress in an appropriate direction since the curvature changes drastically. The Figure also shows that significant progress is made in those early iterations. However, as the slope decreases so does the amount of progress per iteration and little improvement occurs over the bulk of the iterations. Figure 3b shows a close up of the final parts of the training where the solution maneuvers through a valley to the local minimum within a trough.

Cyclical learning rates are well suited for training when the loss topology takes this form. The learning rate initially starts small to allow convergence to begin. As the network traverses the flat valley, the learning rate is large, allowing for faster progress through the valley. In the final stages of the training, when the training needs to settle into the local minimum (as seen in Figure 3b), the learning rate is once again reduced to its original small value.

[1]Figure reproduced from Smith (2017) with permission.

[2]Figure reproduced from Goodfellow et al. (2014) with permission.

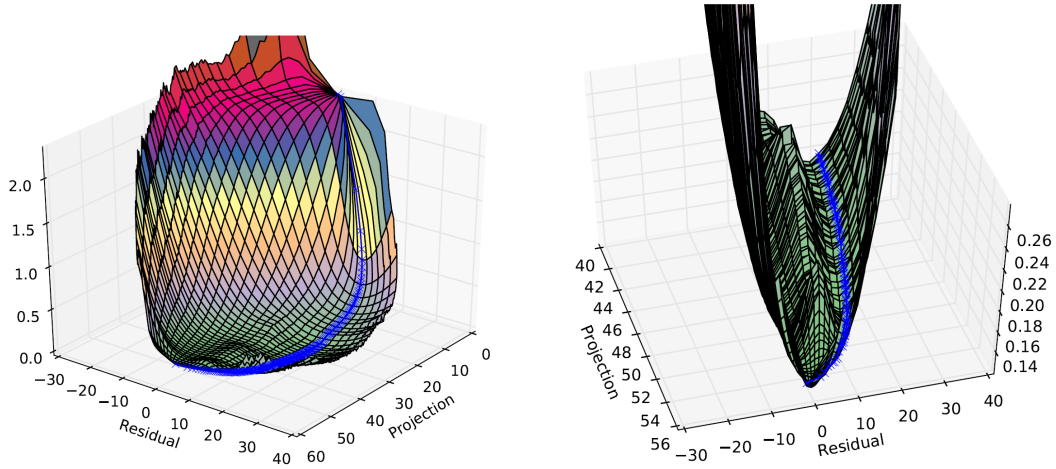

(a) Visualization of how training transverses a loss function topology.

(b) A close up of the end of the training for the example in Figure 3a.

Figure 3: The 3-D visualizations from Goodfellow et al. (2014).

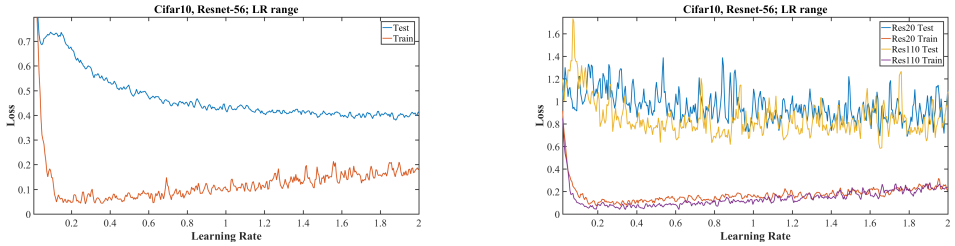

(a) LR range test for Resnet-56.

(b) LR range tests for Resnet-20 and Resnet-110.

Figure 4: Evidence of regularization with large learning rates: decreasing generalization error as the learning rate increases from 0.3 to 1.5.

4 Large Learning Rate Regularization

In our experiments, we only observed super-convergence with large learning rates. In this section, we present evidence that large rates reduce the generalization error, which implies that large learning rates regularize networks.

The LR range test reveals evidence of regularization through results shown in Figure 4a. Figure 4a shows an increasing training loss and decreasing test loss while the learning rate increases from approximately 0.2 to 2.0 when training with the Cifar-10 dataset and a Resnet-56 architecture, which implies that regularization is occurring while training with these large learning rates. Similarly, Figure 4b presents the training and test loss curves for Resnet-20 and Resnet-110, where one can see the same decreasing generalization error. In addition, we ran the LR range test on residual networks with l layers, where $l = 20 + 9n$; for $n = 0, 1, ...10$ and obtained similar results.

There is additional evidence that large learning rates are regularizing the training. As shown in Figure 1a, the final test accuracy results from a super-convergence training is demonstrably better than the accuracy results from a typical training method. In the literature, this type of improvement in the final training accuracy is often taken as evidence of regularization.

5 Estimating Optimal Learning Rates

Gradient or steepest descent is an optimization method that uses the slope as computed by the derivative to move in the direction of greatest negative gradient to iteratively update a variable. That

is, given an initial point x_0, gradient descent proposes the next point to be:

$$x = x_0 - \epsilon \bigtriangledown_x f(x) \tag{1}$$

where ϵ is the step size or learning rate . If we denote the parameters in a neural network (i.e., weights) as $\theta \in R^N$ and $f(\theta)$ is the loss function, we can apply gradient descent to learn the weights of a network; i.e., with input x, a solution y, and non-linearity σ:

$$y = f(\theta) = \sigma(W_l \sigma(W_{l-1} \sigma(W_{l-2} ... \sigma(W_0 x + b_0) ... + b_l) \tag{2}$$

where $W_l \in \theta$ are the weights for layer l and $b_l \in \theta$ are biases for layer l.

The Hessian-free optimization method (Martens, 2010) suggests a second order solution that utilizes the slope information contained in the second derivative (i.e., the derivative of the gradient $\bigtriangledown_\theta f(\theta)$). From Martens (2010), the main idea of the second order Newton's method is that the loss function can be locally approximated by the quadratic as:

$$f(\theta) \approx f(\theta_0) + (\theta - \theta_0)^T \bigtriangledown_\theta f(\theta_0) + \frac{1}{2}(\theta - \theta_0)^T H (\theta - \theta_0) \tag{3}$$

where H is the Hessian, or the second derivative matrix of $f(\theta_0)$. Writing Equation 1 to update the parameters at iteration i as:

$$\theta_{i+1} = \theta_i - \epsilon \bigtriangledown_\theta f(\theta_i) \tag{4}$$

allows Equation 3 to be re-written as:

$$f(\theta_i - \epsilon \bigtriangledown_\theta f(\theta_i)) \approx f(\theta_i) + (\theta_{i+1} - \theta_i)^T \bigtriangledown_\theta f(\theta_i) + \frac{1}{2}(\theta_{i+1} - \theta_i)^T H (\theta_{i+1} - \theta_i) \tag{5}$$

In general it is not feasible to compute the Hessian matrix, which has $\Omega(N^2)$ elements, where N is the number of parameters in the network, but it is unnecessary to compute the full Hessian. The Hessian expresses the curvature in all directions in a high dimensional space, but the only relevant curvature direction is in the direction of steepest descent that SGD will traverse. This concept is contained within Hessian-free optimization, as Martens (2010) suggests a finite difference approach for obtaining an estimate of the Hessian from two gradients:

$$H(\theta) = \lim_{\delta \to 0} \frac{\bigtriangledown f(\theta + \delta) - \bigtriangledown f(\theta)}{\delta} \tag{6}$$

where δ should be in the direction of the steepest descent. The AdaSecant method (Gulcehre et al., 2014; 2017) builds an adaptive learning rate method based on this finite difference approximation as:

$$\epsilon^* \approx \frac{\theta_{i+1} - \theta_i}{\bigtriangledown f(\theta_{i+1}) - \bigtriangledown f(\theta_i)} \tag{7}$$

where ϵ^* represents the optimal learning rate for each of the neurons. Utilizing Equation 4, we rewrite Equation 7 in terms of the differences between the weights from three sequential iterations as:

$$\epsilon^* = \epsilon \ \frac{\theta_{i+1} - \theta_i}{2\theta_{i+1} - \theta_i - \theta_{i+2}} \tag{8}$$

where ϵ on the right hand side is the learning rate value actually used in the calculations to update the weights. Equation 8 is an expression for an adaptive learning rate for each weight update. We borrow the method in Schaul et al. (2013) to obtain an estimate of the global learning rate from the weight specific rates by summing over the numerator and denominator, with one minor difference. In Schaul et al. (2013) their expression is squared, leading to positive values – therefore we sum the absolute values of each quantity to maintain positivity (using the square root of the sum of squares of the numerator and denominator of Equation 8 leads to similar results).

For illustrative purposes, we computed the optimal learning rates from the weights of every iteration using Equation 8 for two runs: first when the learning rate was a constant value of 0.1 and second with CLR in the range of $0.1 - 3$ with a stepsize of 5,000 iterations. Since the computed learning rate exhibited rapid variations, we computed a moving average of the estimated learning rate as $LR = \alpha\epsilon^* + (1 - \alpha)LR$ with $\alpha = 0.1$ and the results are shown in Figure 5a for the first 300 iterations. This curve qualitatively shows that the optimal learning rates should be in the range of 2 to 4 for this architecture. In Figure 5b, we used the weights as computed every 10 iterations and ran the

learning rate estimation for 10,000 iterations. An interesting divergence happens here: when keeping the learning rate constant, the learning rate estimate initially spikes to a value of about 3 but then drops down near 0.2. On the other hand, the learning rate estimate using CLR remains high until the end where it settles down to a value of about 0.5. In addition to providing some support for using large learning rates, these learning rate estimates support the hypothesis that the final solutions and the paths taken to these solutions are different. The code necessary to replicate this work will be made available upon publication.

In this paper we do not perform a full evaluation of the effectiveness of this technique as it is tangential to the theme of this work. We only use this method here to demonstrate that training with large learning rates are indicated by this approximation. We leave a full assessment and tests of this method to estimate optimal adaptive learning rates as future work.

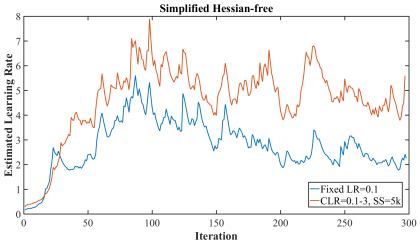

(a) Estimated learning rates computed from the weights at every iteration for 300 iterations.

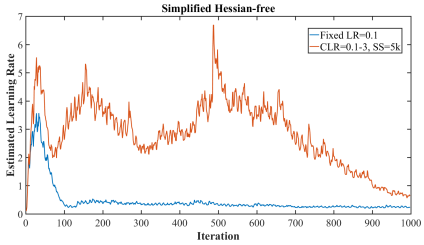

(b) Estimated learning rates computed from the weights at every 10 iterations for 10,000 iterations.

Figure 5: Estimated learning rate from the simplified Hessian-free optimization (see text for additional information).

6 Experiments and Analysis

This section highlights a few of our more significant experiments, and further experiments are illustrated in the Supplemental Section. Furthermore, the Supplemental Section provides details of our architecture.

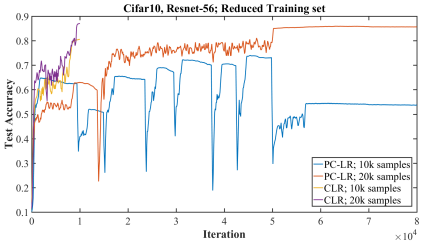

(a) Comparison of test accuracies for Cifar-10 with limited training samples.

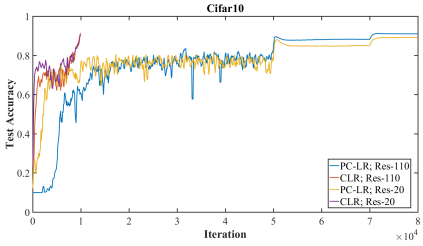

(b) Comparison of test accuracies for Resnet-20 and Resnet-110.

Figure 6: Comparisons of super-convergence to typical training outcome with piecewise constant learning rate schedule.

6.1 Where super-convergence occurs

Figure 6a provides a comparison of super-convergence with a reduced number of training samples. When the amount of training data is limited, the gap in performance between the result of standard training and super-convergence increases. With a standard learning rate schedule (here "standard" means a piecewise constant schedule), the training encounters difficulties and diverges along the way. On the other hand, a network trained with specific CLR parameters exhibits super-convergence and trains without difficulties. The highest accuracies attained using standard learning rate schedules are listed in Table 1 and super-convergence test accuracy is 1.2%, 5.2%, and 9.2% better for 50,000, 20,000, and 10,000 training cases, respectively. This increase in performance gap as the number of

# training samples	Policy (Range)	BN MAF	Total Iterations	Accuracy (%)
40,000	PC-LR=0.35	0.999	80,000	89.1
40,000	CLR (0.1-3)	0.95	10,000	91.1
30,000	PC-LR=0.35	0.999	80,000	85.7
30,000	CLR (0.1-3)	0.95	10,000	89.6
20,000	PC-LR=0.35	0.999	80,000	82.7
20,000	CLR (0.1-3)	0.95	10,000	87.9
10,000	PC-LR=0.35	0.999	80,000	71.4
10,000	CLR (0.1-3)	0.95	10,000	80.6
50,000	CLR (0.1-3.5)	0.95	10,000	92.1
50,000	CLR (0.1-3)	0.95	10,000	92.4
50,000	CLR (0.1-2.5)	0.95	10,000	92.3
50,000	CLR (0.1-2)	0.95	10,000	91.7
50,000	CLR (0.1-1.5)	0.95	10,000	90.9
50,000	CLR (0.1-1)	0.95	10,000	91.3
50,000	CLR (0.1-3)	0.97	20,000	92.7
50,000	CLR (0.1-3)	0.95	10,000	92.4
50,000	CLR (0.1-3)	0.93	8,000	91.7
50,000	CLR (0.1-3)	0.90	6,000	92.1
50,000	CLR (0.1-3)	0.85	4,000	91.1
50,000	CLR (0.1-3)	0.80	2,000	89.7

Table 1: Comparison of final accuracy results for various training regimes of Resnet-56 on Cifar-10. BN MAF is the value use for the $moving\_average\_fraction$ parameter with batch normalization. PC-LR is a standard piecewise constant learning rate policy described in Section 2 with an initial learning rate of 0.35.

training samples decreases indicates that super-convergence becomes more beneficial as the training data becomes more limited.

We also ran experiments with Resnets with a number of layers in the range of 20 to 110 layers; that is, we ran experiments on residual networks with l layers, where $l = 20 + 9n$; for $n = 0, 1, ...10$. Figure 6b illustrates the results for Resnet-20 and Resnet-110, for both a typical (piecewise constant) training regime with a standard initial learning rate of 0.35 and for CLR with a stepsize of 10,000 iterations. For this entire range of architecture depths, super-convergence was possible. The accuracy increase due to super-convergence appears to be greater for the shallower architectures (Resnet-20: CLR 90.4% versus piecewise constant LR schedule 88.6%) than for the deeper architectures (Resnet-110: CLR 92.1% versus piecewise constant LR schedule 91.0%).

We ran a series of experiments with a variety of ranges for CLR. Table 1 shows the results for maximum learning rate bounds from 1.0 to 3.5. These experiments show that a maximum learning rate of 1 was too small and a value of approximately 3 performed well. Our test with the minimum learning rate bound below 0.1 slightly decreased the performance of the network. Hence, most of our experiments were performed with the range of 0.1 to 3.

We tested the effect of batch normalization on super-convergence. Initially, we found that having $use\_global\_stats : true$ in the test phase, prevents super-convergence but when using $use\_global\_stats : false$ in both train and test phases, super-convergence occurs. We realized this was because using the default value of $moving\_average\_fraction = 0.999$ is only appropriate for the typical, very long training times. However, when a network is trained very quickly, as with super-convergence, the default value of the $moving\_average\_fraction$ does not update the accumulated global statistics quickly enough. Since the network is trained for many fewer iterations during super-convergence, we found that the smaller values listed in Table 1 (column BN MAF) were more appropriate for $moving\_average\_fraction$.

We ran a variety of other experiments in which super-convergence continued to occur and those results are reported in the supplemental materials. We ran experiments with Cifar-100 that demonstrated the super-convergence phenomenon. We found that adding dropout to the architecture still permitted super-convergence and improved the results a small amount. Our experiments also investigated whether adaptive learning rate methods in a piecewise constant training regime would learn to adap-

tively use a large learning rate to improve performance. We tested Nesterov momentum (Sutskever et al., 2013; Nesterov, 1983), AdaDelta (Duchi et al., 2011), AdaGrad (Zeiler, 2012), and Adam (Kingma & Ba, 2014) on Cifar-10 with the Resnet-56 architecture but none of these methods speed up the training process in a similar fashion to super-convergence. We also tried these methods with CLR with appropriate bounds and found super-convergence happens for AdaDelta, AdaGrad and Nesterov momentum but we were unable to achieve super-convergence with Adam. In addition, we investigated the effect of momentum. We ran experiments with momentum in the range of $0.80 - 0.95$ and found momentums between $0.8 - 0.9$ yield a higher final test accuracy. We illustrate the results of these experiments in the supplemental materials.

6.2 And where super-convergence does not occur

Super-convergence does not happen with the majority of datasets, architectures, and hyper-parameter settings. We acknowledge that even though we did not observe super-convergence in many experiments, it does not necessarily mean that the super-convergence phenomenon is impossible in those cases but only that we did not find a way to induce it.

Here we will list some of the experiments we tried that failed to produce the super-convergence behavior. Although experiments showed the super-convergence phenomenon with the Cifar-10 and Cifar-100 datasets, super-convergence did not occur when training with the Imagenet dataset. We ran Imagenet experiments with Resnets, ResNeXt, GoogleNet/Inception, VGG, AlexNet, and Densenet without success. Other architectures we tried with Cifar-10 that did not show super-convergence capability included ResNeXt, Densenet, and a bottleneck version of Resnet. Please see the Supplemental Materials for more information.

Next, we were interested in what minimal changes we could make to the Resnet architecture that move the design outside the super-convergence realm. We found that super-convergence works best with weight decay=0.0001 and did not work with values an order of magnitude larger (details are in the supplemental materials).

7 Discussion

We presented empirical evidence for a previously unknown phenomenon that we name super-convergence. In super-convergence, residual networks are trained with large learning rates in an order of magnitude fewer iterations and to a higher final test accuracy than when using a piecewise constant training regime. We provided evidence that large learning rates regularize the training leading to the higher performance of super-convergence. Particularly noteworthy is the observation that the gains from super-convergence increase as the available labeled training data becomes more limited. Furthermore, this paper describes a simplification of the Hessian-free optimization method that we used for estimating learning rates. We show that this method provides additional support for using large learning rates and that the paths taken to a final solution are different between the standard methods and cyclical learning rates with large learning rates.

We believe that a deeper study of super-convergence may lead to a better understanding of deep networks, their optimization, and their loss function landscape.

References

Léon Bottou. Stochastic gradient descent tricks. In *Neural networks: Tricks of the trade*, pp. 421–436. Springer, 2012.

Pratik Chaudhari, Anna Choromanska, Stefano Soatto, and Yann LeCun. Entropy-sgd: Biasing gradient descent into wide valleys. *arXiv preprint arXiv:1611.01838*, 2016.

John Duchi, Elad Hazan, and Yoram Singer. Adaptive subgradient methods for online learning and stochastic optimization. *Journal of Machine Learning Research*, 12(Jul):2121–2159, 2011.

Ian Goodfellow, Yoshua Bengio, and Aaron Courville. *Deep learning*. MIT Press, 2016.

Ian J Goodfellow, Oriol Vinyals, and Andrew M Saxe. Qualitatively characterizing neural network optimization problems. *arXiv preprint arXiv:1412.6544*, 2014.

Caglar Gulcehre, Marcin Moczulski, and Yoshua Bengio. Adasecant: robust adaptive secant method for stochastic gradient. *arXiv preprint arXiv:1412.7419*, 2014.

Caglar Gulcehre, Jose Sotelo, Marcin Moczulski, and Yoshua Bengio. A robust adaptive stochastic gradient method for deep learning. *arXiv preprint arXiv:1703.00788*, 2017.

Kaiming He, Xiangyu Zhang, Shaoqing Ren, and Jian Sun. Deep residual learning for image recognition. In *Proceedings of the IEEE Conference on Computer Vision and Pattern Recognition*, pp. 770–778, 2016.

Daniel Jiwoong Im, Michael Tao, and Kristin Branson. An empirical analysis of deep network loss surfaces. *arXiv preprint arXiv:1612.04010*, 2016.

Diederik Kingma and Jimmy Ba. Adam: A method for stochastic optimization. *arXiv preprint arXiv:1412.6980*, 2014.

Ilya Loshchilov and Frank Hutter. Sgdr: stochastic gradient descent with restarts. *arXiv preprint arXiv:1608.03983*, 2016.

James Martens. Deep learning via hessian-free optimization. In *Proceedings of the 27th International Conference on Machine Learning (ICML-10)*, pp. 735–742, 2010.

Yurii Nesterov. A method of solving a convex programming problem with convergence rate o (1/k2). In *Soviet Mathematics Doklady*, volume 27, pp. 372–376, 1983.

Tom Schaul, Sixin Zhang, and Yann LeCun. No more pesky learning rates. *ICML (3)*, 28:343–351, 2013.

Leslie N. Smith. No more pesky learning rate guessing games. *arXiv preprint arXiv:1506.01186*, 2015.

Leslie N. Smith. Cyclical learning rates for training neural networks. In *Proceedings of the IEEE Winter Conference on Applied Computer Vision*, 2017.

Ilya Sutskever, James Martens, George E Dahl, and Geoffrey E Hinton. On the importance of initialization and momentum in deep learning. *ICML (3)*, 28:1139–1147, 2013.

Matthew D Zeiler. Adadelta: an adaptive learning rate method. *arXiv preprint arXiv:1212.5701*, 2012.

A SUPPLEMENTAL MATERIAL

This Section contains the details of the experiments that were carried out in support of this research. It also contains results for several of our more interesting experiments that did not fit in the main text of the paper.

A.1 DATASETS, ARCHITECTURES, AND HYPER-PARAMETERS

All of the experiments were run with Caffe (downloaded October 16, 2016) using CUDA 7.0 and Nvidia's CuDNN. These experiments were run on a 64 node cluster with 8 Nvidia Titan Black GPUs, 128 GB memory, and dual Intel Xeon E5-2620 v2 CPUs per node and we utilized the multi-gpu implementation of Caffe.

The Resnet-56 architecture used consists of three stages. Within each stage, the same residual block structure is sequentially repeated. This structure is given in Table 2. Between stages, a different residual block structure is used to reduce the spatial dimension of the channels. Table 3 shows this structure. The overall architecture is described in Table 4. Following the Caffe convention, each Batch Norm layer was followed by a scaling layer to achieve true batch normalization behavior. This and the other architectures necessary to replicate this work will be made available upon publication.

Table 2: A residual block which forms the basis of a Residual Network.

Layer	Parameters
Conv Layer 1	padding = 1 kernel = 3x3 stride = 1 channels = $numChannels$
Batch Norm 1	moving_average_fraction=0.95
ReLu 1	—
Conv Layer 2	padding = 1 kernel = 3x3 stride = 1 channels = $numChannels$
Batch Norm 2	moving_average_fraction=0.95
Sum (BN2 output with original input)	—
ReLu 2	—

Table 3: A modified residual block which downsamples while doubling the number of channels.

Layer	Parameters
Conv Layer 1	padding = 1 kernel = 3x3 stride = 2 channels = $numChannels$
Batch Norm 1	moving_average_fraction=0.95
ReLu 1	—
Conv Layer 2	padding = 1 kernel = 3x3 stride = 1 channels = $numChannels$
Batch Norm 2	moving_average_fraction=0.95
Average Pooling (of original input)	padding = 0 kernel = 3x3 stride = 2
Sum (BN2 output with AvgPool output)	—
ReLu 2	—
Concatenate (with zeroes)	channels = 2*$numChannels$

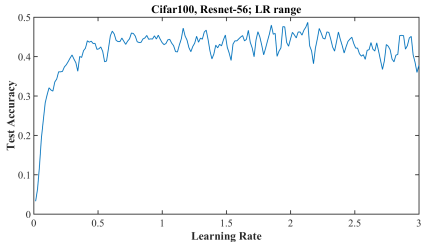

(a) Learning rate range test.

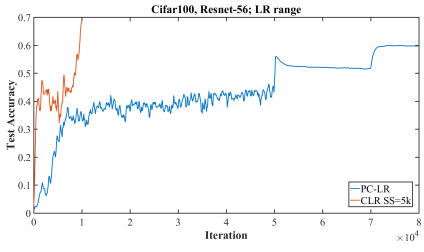

(b) Comparison of test accuracies for super-convergence to a piecewise constant training regime.

Figure 7: Comparisons for Cifar-100, Resnet-56 of super-convergence to typical (piecewise constant) training regime.

Table 4: Overall architecture for ResNet-56.

Layer/Block Type	Parameters
Conv Layer	padding = 1 kernel = 3x3 stride = 2 channels = 16
Batch Norm	moving_average_fraction=0.95
ReLU	—
ResNet Standard Block x9	$numChannels$ = 16
ResNet Downsample Block	$numChannels$ = 16
ResNet Standard Block x8	$numChannels$ = 32
ResNet Downsample Block	$numChannels$ = 32
ResNet Standard Block x8	$numChannels$ = 64
Average Pooling	padding = 0 kernel = 8x8 stride = 1
Fully Connected Layer	—

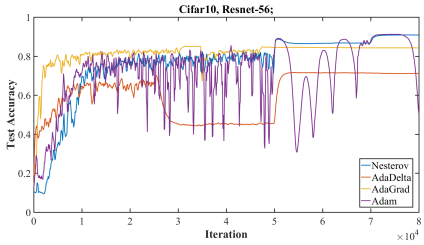

(a) Comparison of test accuracies with various adaptive learning rate methods.

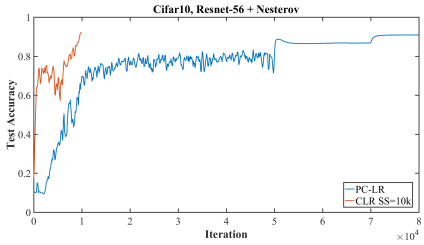

(b) Comparison of test accuracies With Nesterov method.

Figure 8: Comparisons for Cifar-10, Resnet-56 of super-convergence to piecewise constant training regime.

A.2 Additional results

We ran a wide variety of experiments and due to space limitations in the main article, we report some of the more interesting results here that did not fit in the main article.

In the main text we only showed the results of super-convergence for the Cifar-10 dataset. In fact, the super-convergence phenomenon also occurs with Cifar-100, which implies an independence of this

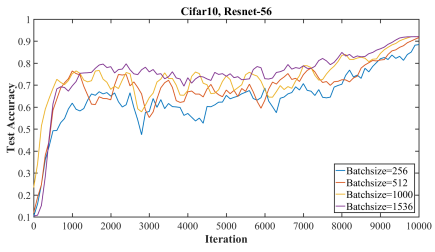

(a) Comparison of test accuracies for Cifar-10, Resnet-56 while varying the total batch sizes.

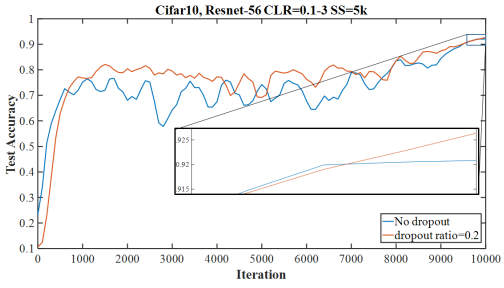

(b) Comparison of test accuracies for super-convergence with and without dropout (dropout ratio=0.2).

Figure 9: Comparisons of super-convergence to piecewise constant training regime.

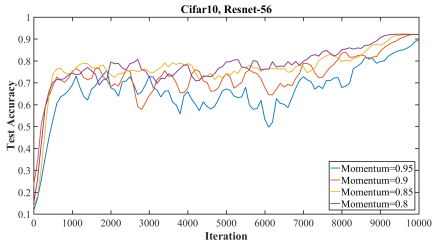

(a) Comparison of test accuracies with three values for momentum.

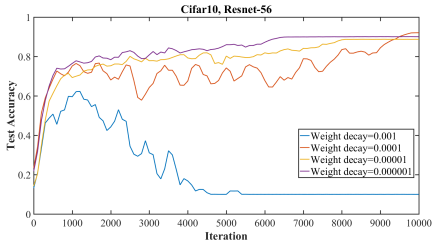

(b) Comparison of test accuracies for super-convergence with various values of weight decay.

Figure 10: Comparisons for Cifar-10, Resnet-56 of super-convergence to typical training regime.

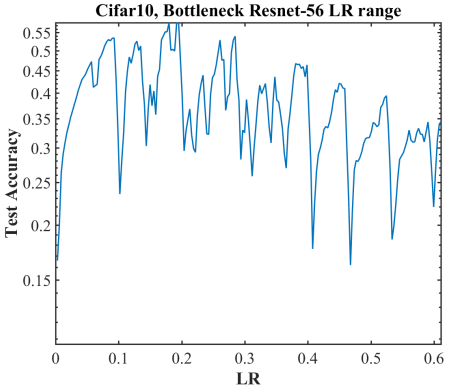

(a) Learning rate range test result with the bottleneck Resnet-56 architecture.

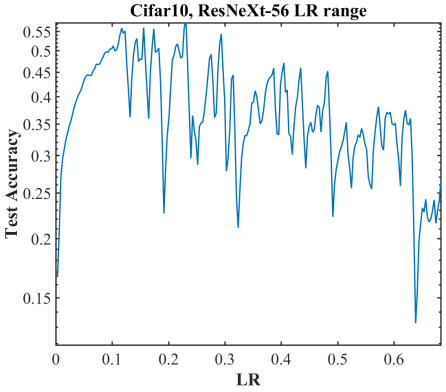

(b) Learning rate range test result with the ResNeXt-56 architecture.

Figure 11: Comparison of learning rate range test results on Cifar-10 with alternate architectures.

phenomenon on the number of classes. Figure 7a shows the results of the LR range test for Resnet-56 with the Cifar-100 training data. The curve is smooth and accuracy remains high over the entire range from 0 to 3 indicating a potential for super-convergence. An example of super-convergence with Cifar-100 with Resnet-56 is given in Figure 7b, where there is also a comparison to the results from a piecewise constant training regime. Furthermore, the final accuracy for the super-convergence curve is 68.6%, while the accuracy for the piecewise constant method is 59.8%, which is an 8.8% improvement.

As discussed in the main text, we tested various adaptive learning rate methods with Resnet-56 training on Cifar-10 to determine if they are capable of recognizing the need for using very large learning rates. Figure 8a shows the results of this training for Nesterov momentum (Sutskever et al., 2013; Nesterov, 1983), AdaDelta (Duchi et al., 2011), AdaGrad (Zeiler, 2012), and Adam (Kingma & Ba, 2014). We found no sign that any of these methods discovered the utility of large learning rates nor any indication of super-convergence-like behavior. We also ran CLR with these adaptive learning methods and found that Nesterov, AdaDelta, and AdaGrad allowed super-convergence to occur, but we were unable to create this phenomenon with Adam. For example, Figure 8b shows a comparison of super-convergence to a piecewise constant training regime with the Nesterov momentum method. Here super-convergence yields a final test accuracy after 10,000 iterations of 92.1% while the piecewise constant training regime at iteration 80,000 has an accuracy of 90.9%.

The total mini-batch size used in training slightly affects the results, as can be seen in Figure 9a. Table 5 lists the final test accuracy results and shows that the larger the mini-batch size, the better the results. Most of our reported results are with a total mini-batch size of 1,000 and we primarily used 8 GPUs and split the mini-batch eight ways over the GPUs.

Are these mini-batch sizes replicated in the non-CLR tests? It seems like super-convergence only works with hella GPUs

Mini-batch size	Accuracy (%)
1536	92.1
1000	92.4
512	91.7
256	89.5

Table 5: Comparison of accuracy results for various total training batch sizes with Resnet-56 on Cifar-10 using CLR=0.1-3 and stepsize=5,000.

Momentum	Accuracy (%)
0.80	92.1
0.85	91.9
0.90	92.4
0.95	90.7

Table 6: Comparison of accuracy results for various momentum values with Resnet-56 on Cifar-10 using CLR=0.1-3 and stepsize=5,000.

Figure 9b shows a comparison of runs of the super-convergence phenomenon, both with and without dropout. In this case, the dropout ratio was set to 0.2 and the figure shows a small improvement with dropout. We also ran with other values for the dropout ratio and consistently saw small improvements.

In addition, we ran experiments on Resnet-56 on Cifar-10 with modified values for momentum and weight decay to determine if they might hinder the super-convergence phenomenon. Figure 10a shows the results for momentum set to 0.8, 0.85, 0.9, and 0.95 and the final test accuracies are listed in Table 6. These results indicate only a small change in the results, with a setting of 0.9 being a bit better than the other values. In Figure 10b are the results for weight decay values of $10^{-3}, 10^{-4}, 10^{-5}$, and 10^{-6}. In this case, a weight decay value of 10^{-3} prevents super-convergence, while the smaller values do not. This Figure also shows that a weight decay value of 10^{-4} performs well.

We also found numerous examples where a change of architecture prevented super-convergence for Cifar-10. Figure 11a shows an example of the LR range test with a bottleneck version of Resnet. There appears to be a peak from a learning rate of approximately 0.15 but even more pronounced are the large swings in the accuracy from around 0.1 and onward. These oscillations and the decay of accuracy at learning rates greater than 0.1 clearly indicate that one cannot train this network with large learning rates and our experiments confirmed this to be true. We also tried Cifar-10 with the the new ResNeXt architecture and were unable to produce the super-convergence phenomenon. Figure 11b shows an example of the LR range test with this architecture. This result is similar to Figure 11a. There appears to be a peak and large swings in the accuracy from a learning rate of approximately 0.1 . These oscillations and the decay of accuracy at learning rates greater than 0.1 indicate that one cannot train this network with large learning rates. Our experiments with Densenets and all our experiments with the Imagenet dataset for a wide variety of architectures failed to produce the super-convergence phenomenon.